High-Frequency Sensor Data Acquisition System (SDAC) for Flight Control and Aerodynamic Data Collection

Or D. Dantsker*, Renato Mancuso†, Michael S. Selig‡, and Marco Caccamo§

University of Illinois at Urbana–Champaign, Urbana, IL 61801

This paper describes a high-frequency sensor data acquisition system (SDAC) for flight control and aerodynamic data collection research on small to mid-sized unmanned aerial vehicles (UAVs). The system is both low weight and low power, operates at 100 Hz and features: a high-frequency, high-resolution six degree-of-freedom (6-DOF) inertial measurement unit (IMU) with a global positioning system (GPS) receiver, a 3-axis magnetometer, a pitot probe, seven 10-bit analog-to-digital converters (ADC), sixteen 12-bit analog-to-digital converters, a 14-bit analog-to-digital converter, twenty digital input/outputs (I/O), eight pulse width modulation (PWM) signal inputs, a 40 mile downlink transceiver, an open serial and an open CANbus port, and up to 64 GB of onboard storage. The data acquisition system was completely fabricated from commercial-off-the-shelf (COTS) components, which reduced the system cost and implementation time. The SDAC combines the large variety of sensor streams into a unified high-fidelity state data stream that is recorded for later aerodynamics analysis and simultaneously forwarded to a separate processing unit, such as an autopilot.

Nomenclature

ADC	=	analog-to-digital converter
ARF	=	almost ready-to-fly
CANbus	=	controller area network bus
COTS	=	commercial off the shelf
CG	=	center of gravity
DOF	=	degree of freedom
GPS	=	global positioning system
IMU	=	inertial measurement unit
I/O	=	input/output
I2C	=	inter-integrated circuit
PWM	=	pulse width modulation
PPM	=	pulse position modulation
RC	=	radio control
RSSI	=	received signal strength indicator
SPI	=	serial peripheral interface
UART	=	universal asynchronous receiver/transmitter
UAV	=	unmanned aerial vehicle

*Graduate Research Fellow, Department of Aerospace Engineering, AIAA Student Member. dantske1@illinois.edu

†Ph.D. Candidate, Department of Computer Science. rmancus2@illinois.edu

‡Associate Professor, Department of Aerospace Engineering, AIAA Associate Fellow. m-selig@illinois.edu

§Associate Professor, Department of Computer Science. mcaccamo@illinois.edu

I. Introduction

There are a variety of data acquisition systems available that offer the ability to connect multiple sensors and record at various rates. Of these there are a smaller selection that would be suitable for small to mid-sized UAVs. These recording systems are sometimes stand-alone but are often part of a processing unit, such as an autopilot, and highly vary in size, weight, and power consumption.

The UIUC Unmanned Aerial Vehicle Research Lab (UAVRL) and Real Time Systems Laboratory (RTSL) have recently developed a high-frequency sensor data acquisition system (SDAC) for use on small to mid-sized UAVs. The SDAC can combine many sensor streams into a unified high-fidelity state data stream and can passively record and/or simultaneously forward that data stream to a separate processing unit. The data acquisition system is completely fabricated out of COTS components, which reduces both cost and implementation time. The system is small, low weight and low power while operating at 100 Hz. It features a large variety of sensors including a high-frequency, high-resolution 6-DOF IMU with a GPS receiver, a 3-axis magnetometer, a pitot probe, seven 10-bit analog-to-digital converters (ADCs), sixteen 12-bit ADCs, a 14-bit ADC, twenty digital I/Os, eight PWM signal inputs, a 40 mile downlink transceiver, an open serial and an open CANbus port, and up to 64 GB of onboard storage. The handful of ADCs, I/Os and ports allow further expandability. A photograph of the SDAC unit is given in Figure 1.

This paper will first briefly examine commercial and other custom-fabricated research data acquisition systems. The paper will then discuss the background and requirements for the SDAC. After that is a description of the implementation of the system along with its specifications. Results from initial testing are presented and finally conclusions and description of future work are given.

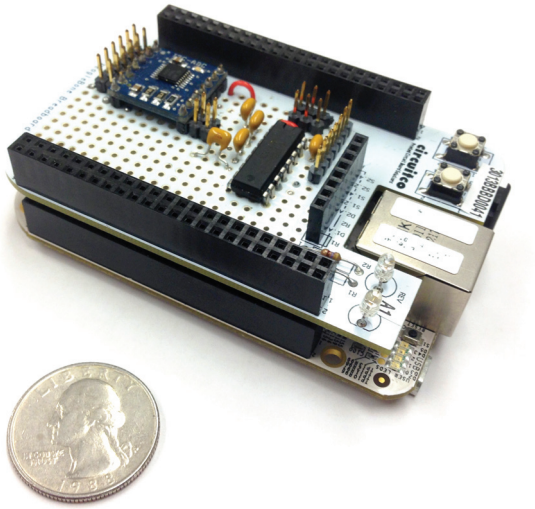

Figure 1. A photograph of the sensor data acquisition system (SDAC) unit.

A. Literature Review of Data Acquisition Systems for Small to Mid-Size UAVs

There are a variety of data acquisition systems and flight control systems that log and process sensor data. In order to properly design and produce a custom solution, existing units had to be evaluated. Existing units examined are separated into commercial products and custom-solution avionics systems and separated into data acquisition systems and flight control systems. It should be noted that this is not a comprehensive study of autopilots or data acquisition systems but rather done to provide a general survey of what is available. That being said, only the sensor handling properties of each unit are presented as that is what the sensor data acquisition systems are intended to do.

There are two types of commercially produced autopilot solutions available: closed-sources and open-source. Closed-source commercial autopilots examined include the Cloud Cap Piccolo II,[1] MicroPilot MP2128g,[2] and Lockheed Martin Kestrel Flight Systems Autopilot v2.4;[3] these closed-source autopilots have been used for many years and often appear referenced in literature: Cloud Cap Piccolo,[4–8] MicroPilot,[9,10] and Kestrel.[11] The specifications for these units are given in Table 1. Open-source commercially-produced autopilots examined include the Paparazzi Lisa/M,[12]

3D Robotics APM 2.6,[13] and Pixhawk PX4 Autopilot;[14] these open-source autopilots are found in literature: Paparazzi Lisa/M,[15] and 3D Robotics APM 2.6.[16] The specifications for these units are given in Table 2.

Next are the commercial data acquisition systems, which include the Crossbow AD2012 data acquisition system,[17] RCAT Systems Industrial UAV datalogger,[18] and Eagle Tree Systems Flight Data Recorder Pro;[19] these units are found in literature: Crossbow AD2012,[20]RCAT Systems Industrial UAV datalogger,[21] and Eagle Tree Systems Flight Data Recorder Pro.[10,22–24] The RCAT System and Eagle Tree Systems units seem to be the only data recording devices currently available with a small enough form factor to allow them to be installed in a small to mid-sized UAV without being a major hindrance. The specifications for these units are given in Table 3.

Finally, several custom-solution avionics systems are examined. In 2003, Higashino and Sakurai developed a testbed vehicle, which included a data acquisition system and associated sensor units, to estimate aerodynamic characteristics.[25] In 2005 Beard et al. developed an autopilot system for small UAVs[26] and in 2006 Christophersen et al. developed the FCS-20 flight control system.[27] NASA's EAV[28] and AirSTAR[29] programs produced testbed platforms that included avionics systems which are able to perform data collection and control. Finally in 2011, Brusov et al. developed the PRP-J5 flight data acquisition system for small UAVs.[30] The specifications for these units are given in Table 4.

Table 1. Closed-source commercially-made autopilot comparison

Unit	Cloud Cap Piccolo II[1]	MicroPilot MP2128g[2]	Kestrel Autopilot v2.4[3]
Sensors			
Inertial sensors	3-axis, ±10 g accelerometer 3-axis, ±300 deg/s gyroscope	3-axis, ±5 g accelerometer 3-axis gyroscope	3-axis, ±10 g accelerometer 3-axis, ±300 deg/s gyroscope
Magnetometers	Add-on supported	Add-on supported	2-axis and 3-axis
Altimeter (barometric)	1 ft resolution	1 ft resolution	0.8 ft resolution
Airspeed (pitot probe)	up to 180 mph	up to 300 mph	0–130 mph
GPS	4 Hz	4 Hz	4 Hz
Digital I/O	16	8	12
Analog inputs	4x 10 bit	32x 24 bit at 5 Hz	3x 12 bit
Other inputs	CANbus	-	4-8 PWM signals, 4 Serial Ports (Std, SPI, I2C)
Data Handling			
Sampling rate	20 Hz	5–30 Hz	100 Hz
Local output	LPT	Serial	Serial
Storage	-	1.5 MB on-board	512 KB on-board
RF link	25 mi	3 mi	15 mi
Estimated cost	$20,000+	$6,000+	$2,500+

Table 2. Open-source commercially-made autopilot comparison

Unit	Paparazzi Lisa/M[12]	3D Robotics APM 2.6[13]	Pixhawk PX4 Autopilot[14]
Sensors			
Inertial sensors	3-axis, ±2-16 g accelerometer 3-axis, ±250-2000 deg/s gyroscope	3-axis, ±2-16 g accelerometer 3-axis, ±250-2000 deg/s gyroscope	3-axis, ±2-16 g accelerometer 3-axis, ±245-2000 deg/s gyroscope
Magnetometers	3-axis ±8 G	3-axis ±8 G	3-axis ±2-12 G
Altimeter (barometric)	1 ft resolution	1 ft resolution	0.3 ft resolution
Airspeed (pitot probe)	Add-on supported	Add-on supported	0–223 mph
GPS	5 Hz	5 Hz	5 Hz
Digital I/O	3	0-12	0
Analog inputs	7	0-12 (same pins as Dig I/O)	2
Other inputs	1x CANbus, 1x SPI, 1x I2C	8 PWM signals, 1x I2C, 2x serial	Up to: 1x PPM sum, 1x RSSI, 6x UART, 2x SPI, 3x I2C, and 1x CANbus
Data Handling			
Sampling rate	50 Hz	50 Hz	50 Hz
Local output	Serial	Serial	Serial
Storage	512 KB on-board	16 MB on-board	2 MB on-board
RF link	Add-on supported	Short	15 mi
Estimated cost	$210	$240+	$200

Table 3. Commercially-made datalogger comparison

Unit	Crossbow AD2012[17]	RCAT Systems Industrial UAV[18]	Eagle Tree Systems Flight Data Recorder Pro[19]
Sensors			
Inertial sensors	-	1-axis, ±8 g accelerometer	2-axis, ±38 g accelerometer
Magnetometers	-	-	-
Altimeter (barometric)	-	8 ft resolution	1 ft resolution
Airspeed (pitot probe)	-	10–290 mph	9–350 mph
GPS	-	1 Hz	10 Hz
Digital I/O	4	-	-
Analog inputs	8x 12 bit	2	2
Other inputs	-	2 Thermocouples, current and voltage measurement, optical RPM measurement	2 Thermocouples, current and voltage measurement, optical RPM measurement, 4 CH PWM measurement
Data Handling			
Sampling rate	1Hz-1kHz	20 Hz	40 Hz
Local output	-	-	-
Storage	2 MB on-board	up to 512 MB SD	10 kB on-board
RF link	-	15 mi	14 mi
Estimated cost	[unknown]	$2,500+	$650–1,500+

Table 4. Custom avionic system solution comparison

Unit	Higashino and Sakurai[25]	Beard et al[26]	FCS-20[27]
Sensors			
Inertial sensors	3-axis, ±5 g accelerometer 3-axis, ±90 deg/s gyroscope	3-axis, ±2 g accelerometer 3-axis, ±500 deg/s gyroscope	3-axis, ±10 g accelerometer 3-axis, ±300 deg/s gyroscope
Magnetometers	-	-	-
Altimeter (barometric)	-	(yes)	(yes)
Airspeed (pitot probe)	(5-hole)	(yes)	(yes)
GPS	-	1 Hz	4 Hz
Digital I/O	-	-	12
Analog inputs	16x 12 bit	16x 12 bit	2x 16 bit, 8x 16 bit
Other inputs	-	4x serial	4x RS-232
Data Handling			
Sampling rate	20Hz	130 Hz	100 Hz
Local output	-	-	-
Storage	12 MB on-board	up to 512 KB on-board	64 MB on-board
RF link	-	3 mi	Supported

Unit	NASA EAV[28]	NASA AirSTAR[29]	Brusov et al. PRP-J5[30]
Sensors			
Inertial sensors	3-axis, ±10 g accelerometer 3-axis, ±200 deg/s gyroscope	3-axis, ±10 g accelerometer 3-axis, ±600 deg/s gyroscope	3-axis, ±2-6 g accelerometer 3-axis, ±300 deg/s gyroscope
Magnetometers	-	-	-
Altimeter (barometric)	-	(yes)	(yes)
Airspeed (pitot probe)	(5-hole)	(yes)	(yes)
GPS	(yes)	5 Hz	-
Digital I/O	-	2	0
Analog inputs	16x 12 bit	48x 16 bit	24x 12 bit
Other inputs	8x PWM signals, 4x RS-232, 8x serial, 1x CANbus	3x serial	4x PWM signals
Data Handling			
Sampling rate	10Hz	50 Hz	100 Hz
Local output	-	-	-
Storage	2x 8 GB CF	up to 512 KB on-board	Up to 512 MB SD
RF link	(yes)	(yes)	-

II. Background and Requirements

The motivation behind developing the sensor data acquisition system was to have a unit that is able to combine many different sensor streams, all arriving in at different times, using different communication protocols, and being generated at different frequencies, into a single unified sensor data stream. The resultant stream would be passively recorded on the SDAC, where sensor data collected would later be used for aerodynamics research. The sensor data acquisition system would also have the ability to simultaneously forward the unified stream to a separate processing unit, such as an autopilot, for flight control, which would alleviate some requirements of that board, in both physical connections and sensor handling.

In terms of general requirements, the SDAC unit should be small enough so that it can be used on small to mid-sized unmanned aerial vehicles. Also, it should be versatile such that it could be used on any platform. The specific sensor handling requirements for the unit were determined by examining previous developed systems[24,31] and by evaluating other existing units, see Section 1.A. The system should yield: 3D linear and angular accelerations, velocities, and position along with GPS location using an IMU; airspeed using a pitot probe and a differential pressure sensor; 3D magnetic field using a magnetometer for heading; control inputs; and control surface deflections using potentiometers. The avionics suite should be able to log and also transmit all of this data to the ground through a high-power transceiver. So the SDAC should include the following sensors and devices: a 6-DOF IMU, a GPS receiver, a 3-axis magnetometer, a pitot probe, ADCs for recording analog devices, such as pressure sensors, thermocouples, and potentiometers; a downlink transceiver, and an on-board storage device, along with the ability to add sensors or other devices later on. All of the devices and sensors mentioned should operate at or above and be acquired at 100 Hz. The acquisition rate value stems from the fact that most actuators operate at 50 Hz and for autopilot inner-loops to yield optimal and accurate control, a sensor sampling frequency of 100 Hz is required. Therefore, the sensor data acquisition system is required to be able to handle the sensor streams being generated by and sent to each of these sensors/devices in real time. Such a requirement defines provisions in both physical hardware specifications and layout and in software design. It is also important to note that the sensor data acquisition system must be fabricated from COTS components to minimize time and cost.

Next, in terms of physical requirements for the system, since the SDAC would be used in small to mid-sized UAVs, it would have inherent size and power limitations. Having such an operating environment means that the final/completed device must have a small footprint in physical size, weight, and power consumption. Minimizing the physical properties of the SDAC yields a decrease in the impact posed on aircraft performance when compared with a non-instrumented aircraft. The same requirement applies to sensors and devices used with the sensor data acquisition system.

That being said, the overwhelming majority of UAVs in the small to mid-size range are propelled by electric propulsion systems. Electric propulsion systems are composed of an electric motor, an electronic speed controller for that motor, and a battery to power the system. However, electric propulsion systems have the inherent disadvantage of producing large varying magnetic fields. The problem with the induced magnetic field is that it interferes with heading measurements taken by the magnetometers. The heading measurements taken by the magnetometer are used as starting points that are filtered using the rotation rate readings generated by the gyroscopes in the IMU.

In order to understand the extent to which electric motors affect state measurement, the UIUC Aero Testbed,[24] which is a large fixed wing electric UAV, was held stationary and test run. The results of the static run can be seen in Figures 2 and 3. Between 200 and 300 sec, the batteries were installed in the aircraft with the motor switch turned off, this led to some slight vibration and motion being created. At around 670 sec, the motor switch was turned on, with power flowing to the motors controller however no power was applied to the motor to rotate. The motor was then run to full speed at 1405 sec and then to zero speed at 1421 sec. Figure 2 shows that there are no magnetic field effects from the accelerometers and the gyroscopes—only noise and motion due to aircraft handling and motor vibration. However, the IMU magnetometer and therefore heading estimation readings were highly influenced by the induced magnetic field. When the motor was turned on, there was a difference of between 0.04 to 0.09 magnetic field units for each axis, from their previous values, which correlates to a heading change of 16 deg. When the motor is run, as can be seen in Fig. 3, the magnetic field readings differed by up to 2.0 magnetic field units from their previous values, which correlates to a heading change of up to 360 deg. It should be noted that the IMU outputs the magnetic field strength in arbitrarily valued magnitude units which sum to approximately 1.3 when only subjected to the Earth's magnetic field.

In order to provide high-fidelity state estimation, the large deviations in attitude caused by the induced magnetic field must be corrected. It was realized that the solution to solving the induced magnetic field problem should come from a combination of hardware and filtering implementation. A second magnetometer should be added to the tail of the aircraft, which due to its distance from the motor in the nose, would be less affected by the induced magnetic field, especially at low throttle settings. As the throttle is advanced, the processing unit handling the unified data

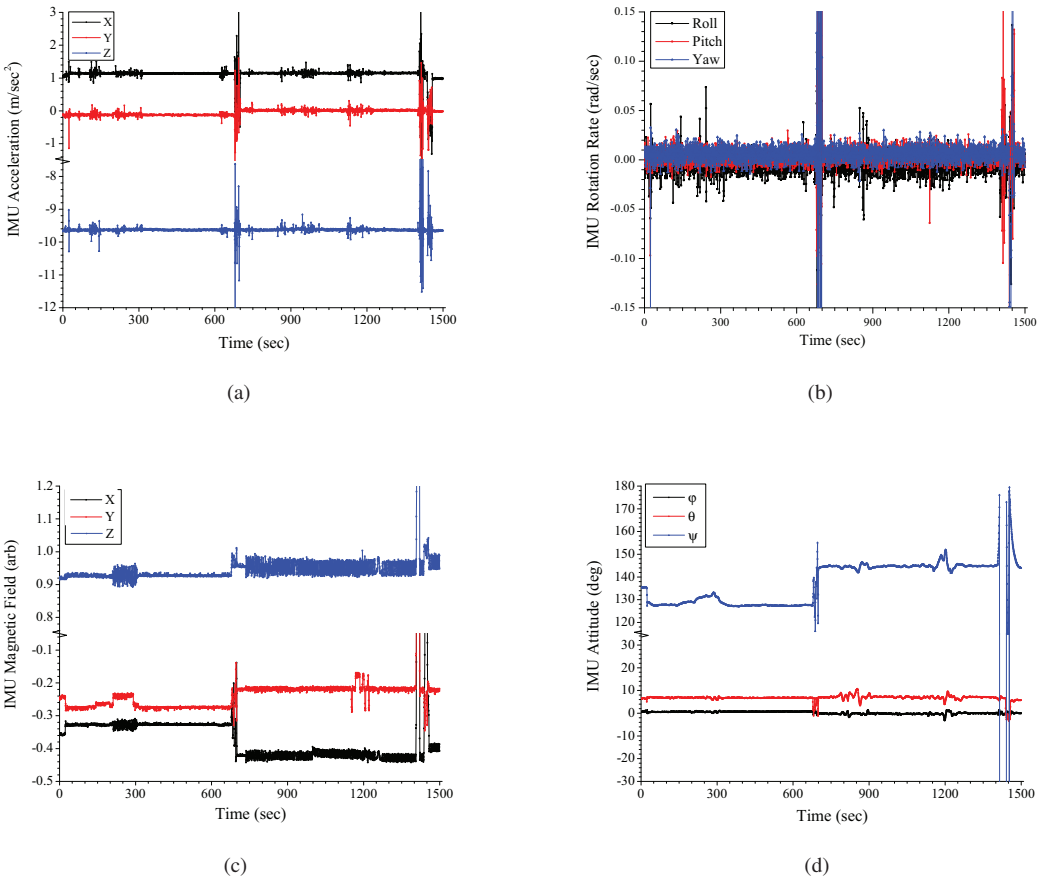

Figure 2. IMU sensor outputs during motor run on UIUC Aero Testbed: a) aircraft body frame accelerations, b) aircraft body frame rotation rates, c) aircraft body frame magnetic field strengths, and d) aircraft attitude.

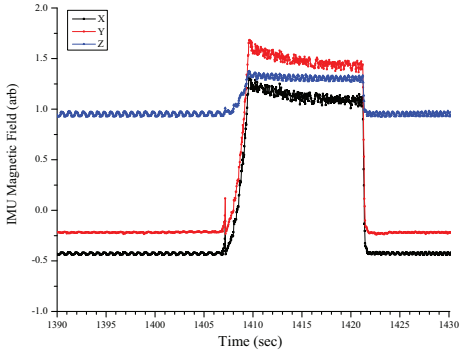

Figure 3. IMU magnetometer readings during a full speed motor run on UIUC Aero Testbed.

stream must trigger and switch to finding the aircraft heading by starting with an unbiased pre-throttled heading angle and integrate from those initial conditions using rotation rate measurements from the gyroscope. Implementing such a system would produce correct heading values independent of the induced magnetic field produced by the electric propulsion system. A description of the algorithm to correct the effects of the induced magnetic field produced and the implementation can be found in Dantsker et al.[32]

With all of the aforementioned factors considered, the sensor data acquisition system must have, in summary:

- Ability to sample, record, and transmit:
  - 3D linear and angular accelerations, velocities, and position along with GPS location using a 6-DOF IMU and GPS receiver
  - Airspeed using a pitot probe and differential pressure sensor
  - 3D magnetic field for determining heading using a magnetometer
  - Control inputs
  - Control surface deflections using potentiometers
- Ability to operate at a frequency of 100 Hz
- All components be COTS
- Minimal impact to the airframe in size, weight, and power consumption
- Ability to correct for the magnetic field induced by an electric propulsion system

III. Implementation and Specifications

The sensor data acquisition system was developed following the requirements set in Section II. The SDAC was developed from COTS components and is plug-and-play, meaning that it could easily be installed into almost any aircraft. The system is able to simultaneously log and transmit at 100 Hz: 3D linear and angular accelerations, velocities, and position along with GPS location; pitot probe airspeed; 3D magnetic field strength and heading; control surface inputs; and control surface deflections. The performance specifications for the SDAC are given in Table 5. A system diagram depicting the main components of the hardware platform is shown in Figure 4. The specifications for all the components used in the sensor data acquisition system are given in Table 6. A description of the software architecture used in the implementation is given in Mancuso et al.[33]

Table 5. Sensor data acquisition unit performance specifications

Sensors	
Inertial sensors	3-axis, ±18 g accelerometer 3-axis, ±300 deg/s gyroscope
Magnetometers	3-axis ±750 mG and 3-axis ±11 G
Altimeter (barometric)	1 ft resolution
Airspeed (pitot probe)	5–180 mph
GPS	120 Hz (IMU assisted)
Digital I/O	20
Analog inputs	7x 10 bit, 16x 12 bit, 1x 14 bit
Other inputs	8 CH PWM measurement, 1x serial port, CANbus
Data Handling	
Sampling rate	100 Hz
Local output	Serial or Ethernet
Storage	Up to 64 GB microSD
RF link	40 mi

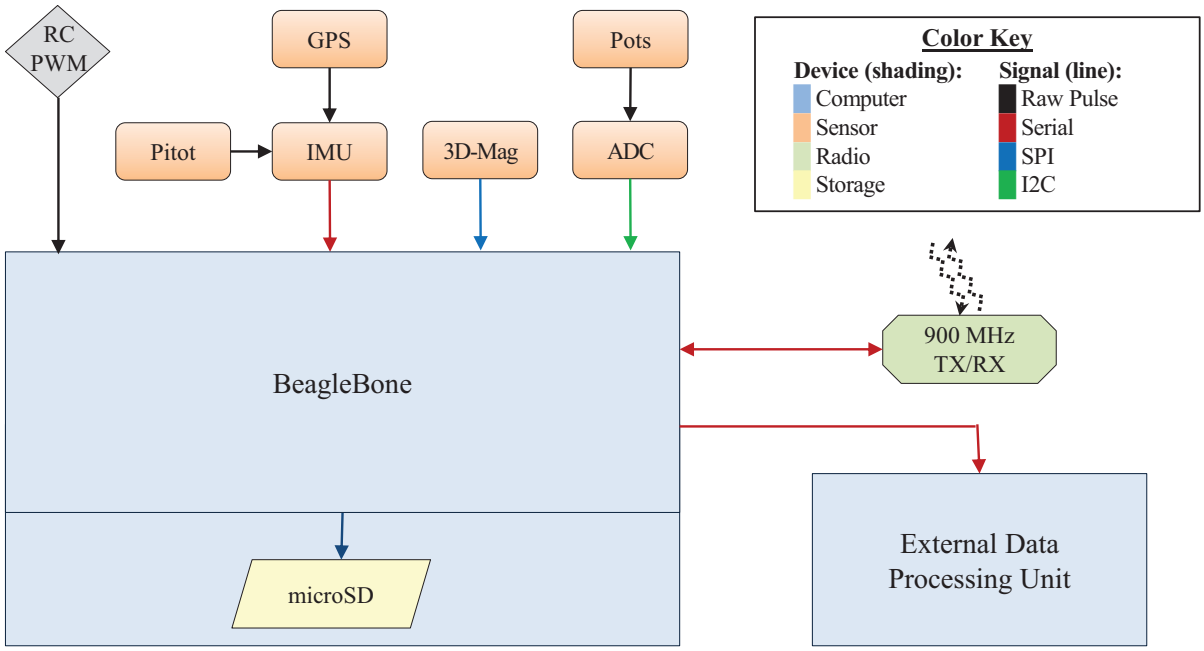

Figure 4. Block diagram of the system

Table 6. Sensor data acquisition unit component specifications

Processing unit	BeagleBone running 32-bit Ubuntu Linux
Sensors	
IMU	XSens Mti-g 6-DOF IMU with Wi-Sys WS3910 GPS Antenna
Airspeed probe	EagleTree Systems pitot-static probe
Airspeed sensor	All Sensors 20cmH2O-D1-4V-MINI differential pressure sensor
Magnetometer	PNI Corp MicroMag 3
Analog-to-digital converters	2x Gravitech 12 bit - 8 Channel ADC
Potentiometers	6x BI Technologies 6127
Power	
Regulators	Castle Creations CCBEC
Batteries	Thunder Power ProLite 2S 450 mAh
Transceiver	Digi 9X Tend 900-MHz card
Data Storage	8GB microSD card
Data Rate	100 Hz

IV. Initial Flight Testing

A radio control aircraft was built and instrumented with the sensor data acquisition system. The aircraft was flown under manual pilot control in order to test the sensor data acquisition unit. This section is separated into several subsections that cover the aircraft setup, ground testing, and flight testing.

A. Aircraft Setup

A radio control model airplane was built to test the sensor data acquisition unit. The aircraft chosen for the task was a Great Planes Avistar Elite,[34] which has a 62.5 in wingspan, 7-8 lb fixed-wing trainer-type airplane. It is equipped with an electric propulsion system that uses a AXI 4120/14 600 W motor,[35] a Castle Creation Phoenix ICE 75 Amp electronic speed controller,[36] and a Thunder Power 14.8 V, 5 Ah lithium polymer battery.[37] The model is actuated using Futaba S3004 ball-bearing standard-torque servos and is controlled by a 2.4 GHz R6014HS spread spectrum receiver.[38] The radio control system is powered by an independent Castle Creations CC BEC regulator, which uses a Thunder Power 7.4 V, 450 mAh lithium polymer battery. The completed flight-ready aircraft is shown in Fig. 5, its physical specifications are given in Table 7, and its airframe component specifications are given in Table 8.

Figure 5. Flight-ready Great Planes Avistar Elite model aircraft.

Table 7. Great Planes Avistar Elite model aircraft physical specifications

Geometric Properties	
Overall Length	55.0 in (1395 mm)
Wingspan	62.5 in (1590 mm)
Wing Area	672 in^2 (43.3 dm^2)
Aspect Ratio	6.62
Inertial Properties	
Weight	
Empty (w/o Battery)	7.53 lb (3.415 kg)
4S LiPo Battery	1.17 lb (0.530 kg)
Gross Weight	8.70 lb (3.945 kg)
Wing Loading	29.8 oz/ft^2 (90.9 gr/dm^2)

Table 8. Great Planes Avistar Elite model aircraft airframe component specifications

Construction	Built-up balsa and plywood structure, aluminum wing tube, aluminum landing gear, ABS canopy, and plastic-film sheeted.
Flight Controls	
Controls	Ailerons (2), elevator, rudder, throttle, and flaps (2)
Transmitter	Futaba T14MZ
Receiver	Futaba R6014HS
Servos	(8) Futaba S3004
Regulator Distribution	Castle Creations CC BEC
Receiver Battery	Thunder ProLite 20c 2S 7.4V 450 mAh
Propulsion	
Motor	AXI 4120/14 Outrunner
ESC	Castle Creation Phoenix ICE 75 Amp Brushless Speed Controller
Propeller	APC 13x8E
Motor Flight Pack	Thunder Power ProPower 30c 4S 14.8 V 5 Ah lithium polymer battery
Flight Time	10–20 min

The sensor data acquisition unit and sensors were installed into the aircraft. Component specifications can be found in Table 6. In chronological order, the following installations were made:

1. The IMU was hard-mounted to the floor of the fuselage at the center of gravity location (see Fig. 6).
2. The sensor data acquisition unit was installed in the center of the fuselage, near and above the IMU (see Figs. 6 and 7).
3. The magnetometer was installed in the tail section of the fuselage (see Figs. 8 and 9).
4. Two potentiometers were installed in the tail section of the fuselage (see Figs. 9 and 10).
5. Four potentiometers were installed in the wings, one per control surface (see Figs. 11 and 12).
6. The pitot probe was mounted on the left wingtip with tubing connecting its pressure taps to the differential pressure sensor also in the left wing (see Figs. 13 and 11).

A view of the center section of the fuselage with the complete wiring is given in Fig. 14.

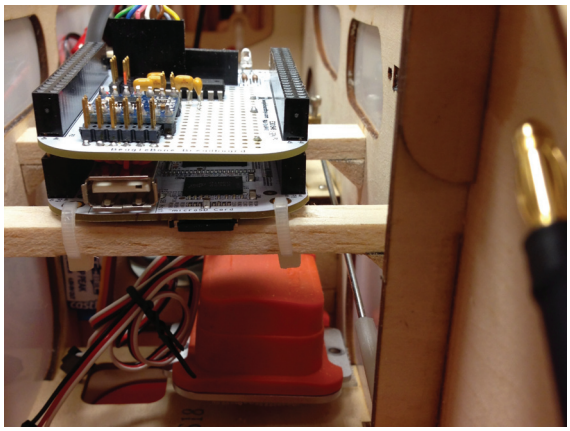

Figure 6. A view from the nose of the aircraft looking rearward showing the SDAC and IMU, which is mounted off-center because the accelerometers are off-centered within the unit.

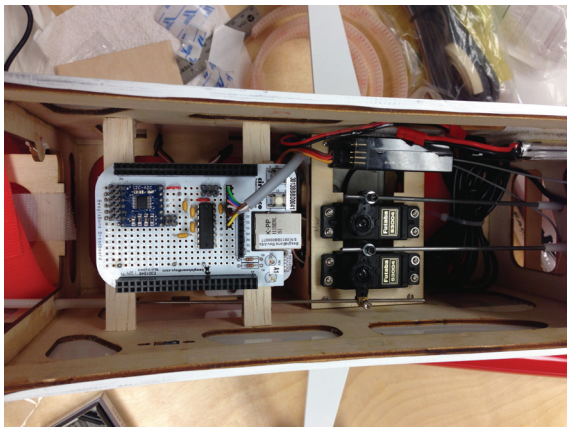

Figure 7. The sensor data acquisition system installed into the fuselage.

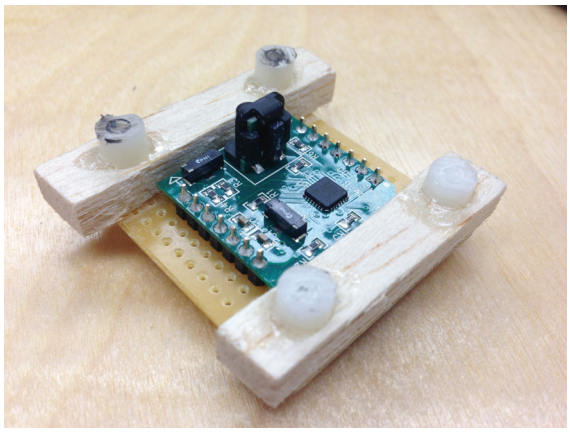

Figure 8. The stand-alone magnetometer on the perfboard mount before installation.

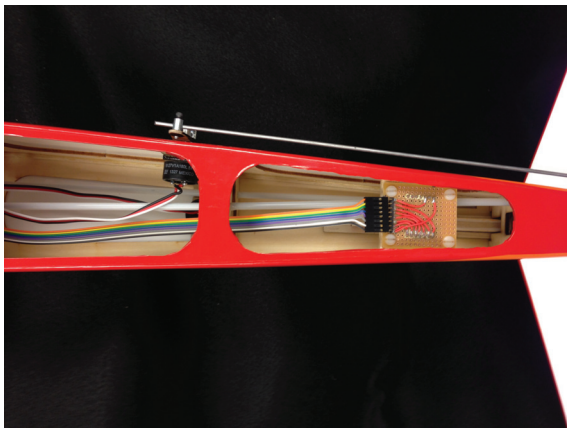

Figure 9. Bottom view of the tail with the coating removed showing the elevator and rudder potentiometers and stand-alone magnetometer installed.

Figure 10. Elevator and rudder with potentiometers and linkages installed.

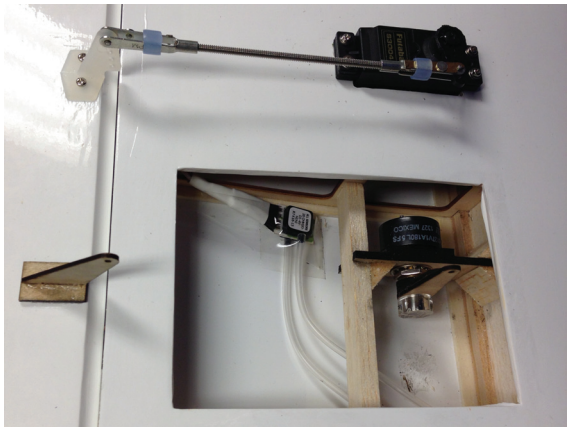

Figure 11. View of the left aileron servo, aileron potentiometer setup (sans pushrod), and pitot probe differential pressure sensor.

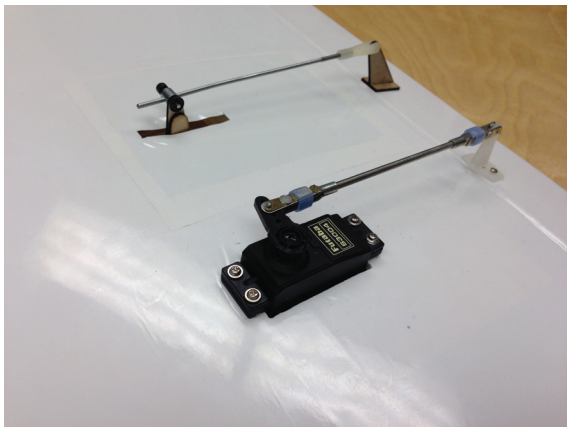

Figure 12. Completed view of the left aileron servo and potentiometer setup with all the linkages installed.

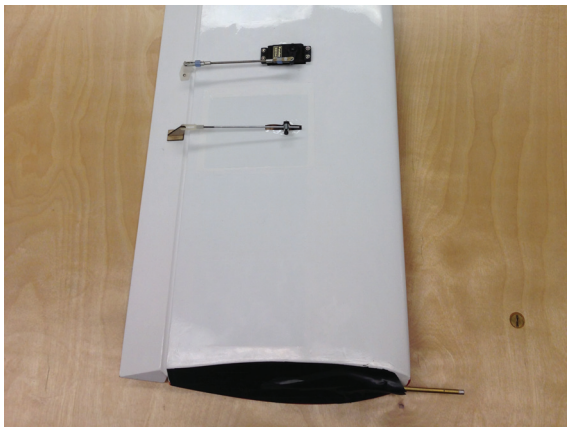

Figure 13. Outboard section of the left wing with the pitot probe, aileron, aileron servo, and aileron potentiometer system in view.

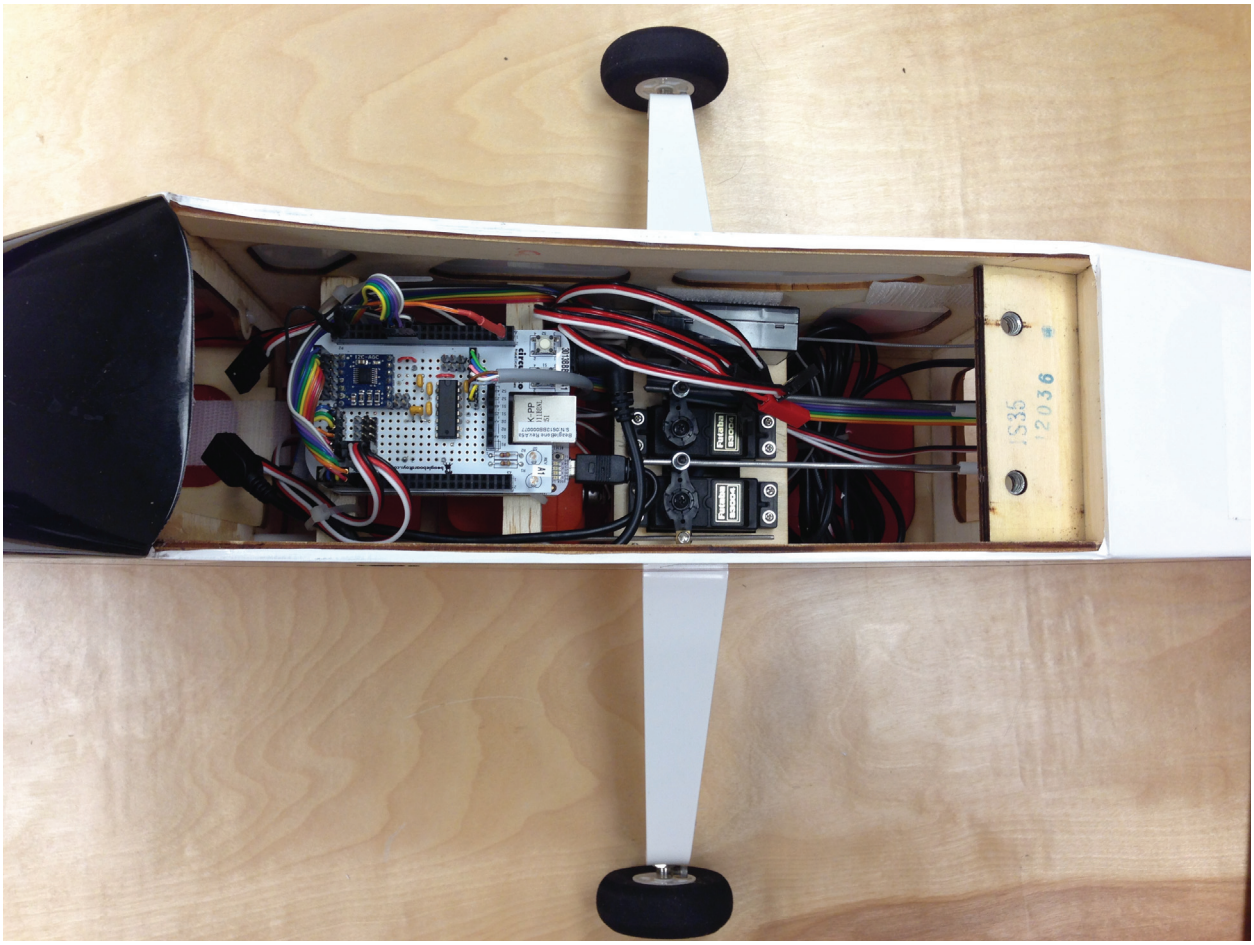

Figure 14. Center section of the fuselage with wiring completed.

B. Ground Testing

The aircraft was placed in an open area. The sensor data acquisition unit was initialized and allowed to sit for 15 min for thermal sensor calibration. After the calibration time, the control inputs for each of the flight controls were cycled with step inputs, one control input at a time: neutral, full, neutral, opposite full, and neutral; 2 sec duration. Figure 15 shows the step control input cycling, which could later be used to calibrate potentiometer values to control inputs.

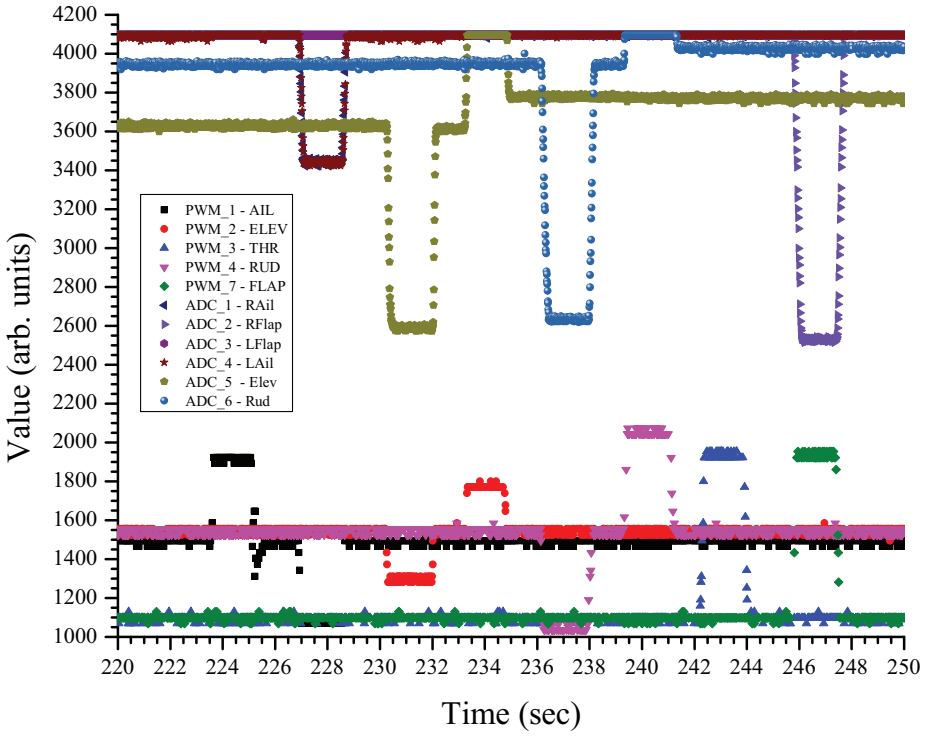

Figure 15. Recorded control inputs and potentiometer measured deflections.

C. Flight Testing

The completed, instrumented Avistar model aircraft was taken to Eli Field in Monticello, IL for flight testing. The aircraft was flown completely manually so that the sensor data acquisition unit could be tested. The unit was initialized and allowed to sit for 15 min so that the sensors could thermally calibrate. Once that occured, the aircraft was placed on the centerline of the runway facing upwind. The aircraft was then throttled up, took off, was flown through a pair of simple traffic patterns, and landed. The entire flight totaled 98 sec from throttle-up to full stop after landing. The flight path of the aircraft is shown in Fig. 16 and the data recorded is shown in Fig. 17.

In the first 7 sec of the recording, the aircraft remained stationary on the runway, which allowed for steady-state measurements to be taken. The plots in Fig. 17 show that there was little to no change in the measurements coming from all of the sensors during this time period. Therefore, it can be assumed that there is minimal interference being induced between any of the subsystems. Then, at 7 sec, the aircraft was throttled-up for takeoff and at 105 sec it completely stopped after landing.

In Fig. 17 (a), the position of the aircraft can be seen with the start position assigned the location (0,0,0); it should be noted that the end location is not the same as the start location because the aircraft rolled to a stop 80 m South-East from the start position. Figure 17 (b) shows the attitude of the aircraft, were ϕ is the roll angle, θ is the pitch angle, and ψ is the heading. The time history of the attitude shows when the aircraft pitching up to takeoff, down to lose altitude before landing, up to flare right before touch-down, and while maneuvering. The changes in heading correlate

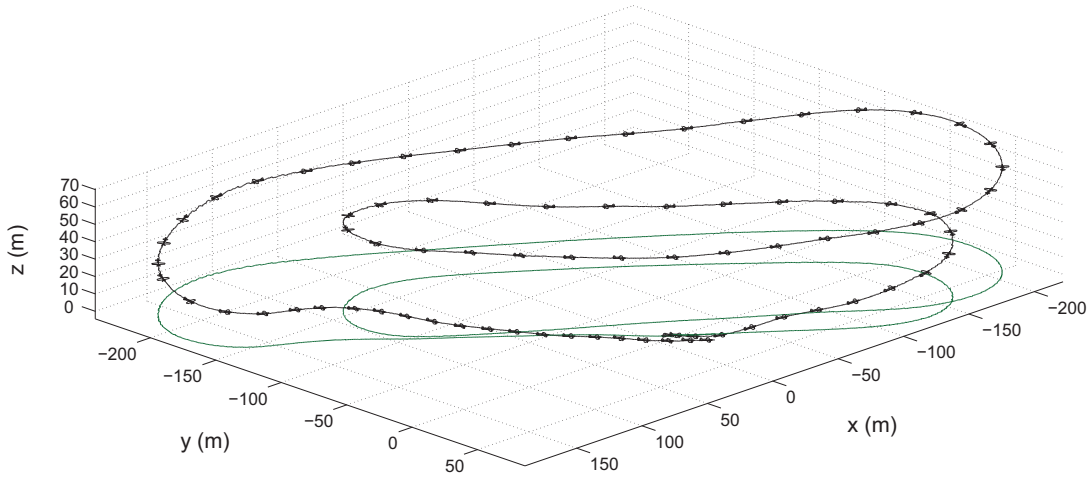

Figure 16. Flight path for initial test flight (the aircraft is drawn three times bigger than the actual size and once every second tangent to the flight path).

with the turns in the traffic pattern seen in (a). It is important to note that when there is a vertical line in the plot, where the heading changes from -180 to 180 deg, the airplane is turning smoothly from heading South-West to South-East, through South, which is represented as both -180 and 180 deg. The roll angles visible in the plot correspond to the roll required for the banked turn and therefore an increase in roll occurs as the turn is initiated and a decrease when the turn is ended.

Figures 17 (c) and (d) show the linear accelerations and rotation rates experienced by the aircraft. The noise seen in these figures are cause by motor/propeller vibration and can be removed by using a low-pass filter. The noise stops between 66 and 88 sec when the motor is turned off before landing in order to lose speed and altitude. There are a few spikes in IMU Z-axis measurements between 91 and 93 sec that correlate to the aircraft bumping on the runway several times during landing. Because the system records at 100 Hz, it can be seen that the aircraft had 2 large bumps with about 1 sec between them followed by a smaller third bump 0.5 sec later, with the airplane finally rolling down the runway after that; this was confirmed with video of the flight taken from the ground.

The horizontal and vertical ground speeds of the aircraft are shown in Fig. 17 (e) and in Fig. 17 (f), the total ground speed and airspeed are plotted. The offset between these speeds are easily accounted for by factoring in the wind. A slight wind during the flight changed direction to the aircraft as the aircraft changed heading. Figure 17 (g) provides a time history of the control inputs given by the pilot. The control inputs for all of the maneuvers described above can be be seen.

Finally, Fig. 17 (h) shows the magnetic field strength as recorded by the IMU and the stand-alone magnetometer. There is a larger offset in magnetic field strength between the magnetometer and IMU when the motor is off as compared to when it is on. The stand-alone magnetometer, which is located in the tail, receives a smaller fraction of the magnetic field induced by the propulsion system than the IMU receives. This difference between the magnetometer reading is magnified when the motor is off.

Therefore, studying the plots in Fig. 17 has shown that the sensor data acquisition system was able to provide continuous high-frequency state data for the entirety of the flight. The sensor plots were able to show fine features of the flight which included the effects of wind and the bumps during landing. Additionally, there were no faults evident in any part of the recording.

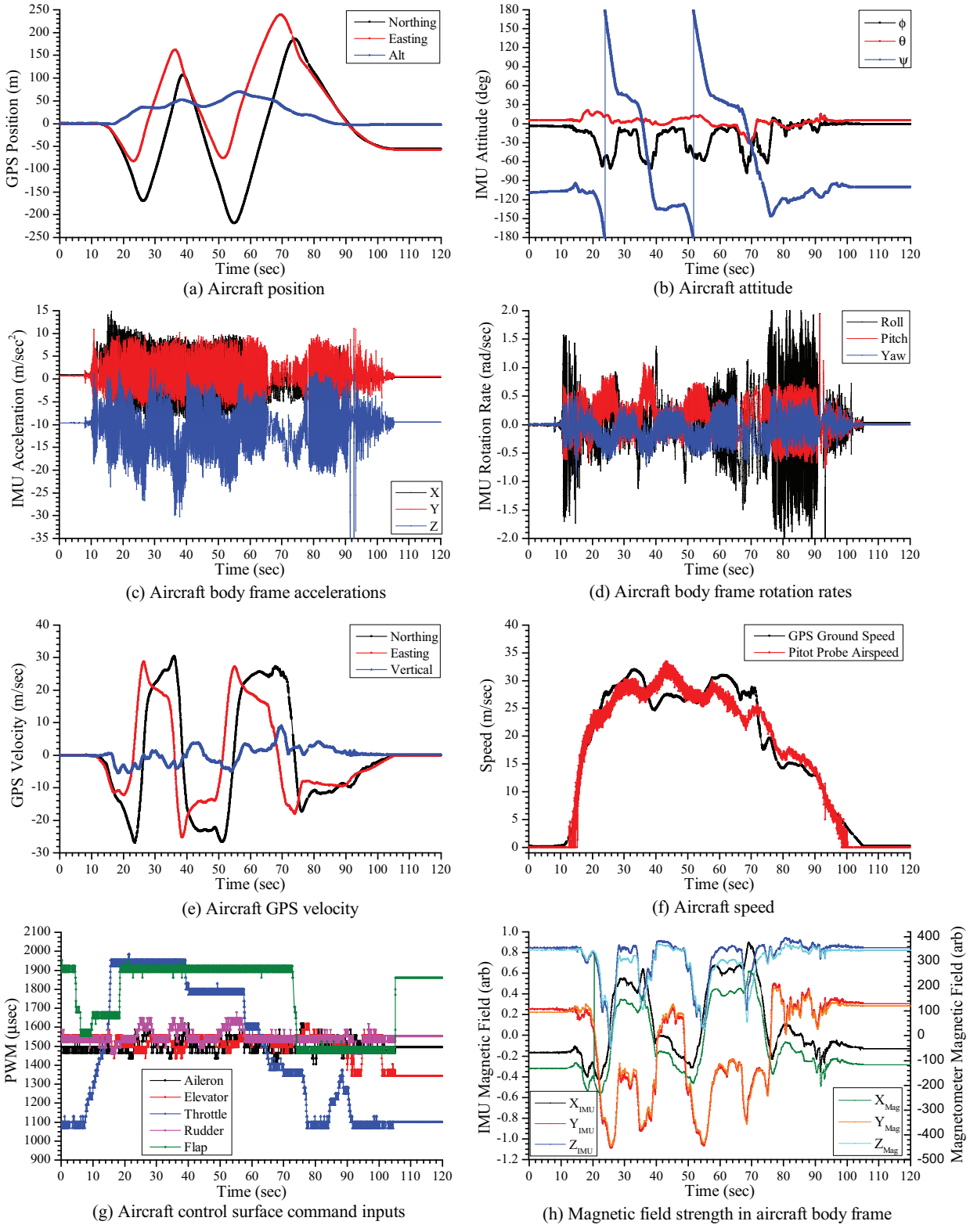

Figure 17. Sensor outputs for initial test flight.

V. Conclusions

A high-frequency sensor data acquisition system (SDAC) was developed for flight control and aerodynamic data collection research on small to mid-sized unmanned aerial vehicles (UAVs). The SDAC combines the large variety of sensor streams into a unified high-fidelity state data stream that is recorded for later aerodynamics analysis and simultaneously forwarded to a separate processing unit, such as an autopilot. The data acquisition system was completely fabricated from COTS components, which reduced both system cost and implementation time. The SDAC has better overall performance than existing systems of similar size. Flight testing has shown that the sensor data acquisition system can provide continuous high-frequency state data for the entirety of a flight with no faults.

Acknowledgments

We would like to thank the Monticello Model Masters RC Club for allowing the use of Eli Field. The material presented in this paper is based upon work supported by the National Science Foundation (NSF) under grant numbers CNS-1302563 and CNS-1219064. Any opinions, findings, and conclusions or recommendations expressed in this publication are those of the authors and do not necessarily reflect the views of the NSF.

References

[1]Cloud Cap Technology, "Cloud Cap Technology – Piccolo II highly integrated UAS Autopilot," https://www.cloudcaptech.com/piccolo_II.shtm, Accessed Oct. 2013.

[2]MicroPilot, "MicroPilot - Products - MP2128g," http://www.micropilot.com/products-mp2128g.htm, Accessed Oct. 2013.

[3]Lockheed Martin, "Kestrel Flight Systems," http://www.lockheedmartin.com/us/products/procerus/kestrel.html, Accessed Nov. 2013.

[4]Uhlig, D., Bhamidipati, K. K., and Neogi, N., "Safety and Reliability Within UAV Construction," Proceedings of the IEEE Digital Avionics System Conference, Portland, OR, 2006.

[5]Dobrokhodov, V. N., Yakimenko, O. A., Jones, K. D., Kaminer, I. I., Bourakov, E., Kitsios, I., and Lizarraga, M., "New Generation of Rapid Flight Test Prototyping System for small Unmanned Air Vehicles," AIAA Paper 2007-6567, AIAA Modeling and Simulation Technologies Conference and Exhibit, Hilton Head, SC, Aug. 2007.

[6]Leong, H. I., Keshmiri, S., and Jager, R., "Evaluation of a COTS Autopilot and Avionics System for UAVs," AIAA Paper 2009-1963, AIAA Infotech@Aerospace, Seattle, WA, Apr. 2009.

[7]Jager, R., *Test and Evaluation of the Piccolo II Autopilot System on a One-Third Scale Yak-54*, Master's thesis, University of Kansas, Department of Aerospace Engineering, Lawrence, KS, 2009.

[8]Czarnomski, M., Spitsberg, R., Dvorak, D., Schultz, R. R., and Semke, W. H., "Benefits of Autopilot Integration for Enhanced UAS Operations," AIAA Paper 2009-1995, AIAA Infotech@Aerospace, Seattle, WA, Apr. 2009.

[9]Motter, M. A., Logan, M. J., French, M. L., and Guerreiro, N. M., "Benefits of Autopilot Integration for Enhanced UAS Operations," AIAA Paper 2006-3305, Aerodynamic Measurement Technology and Ground Testing Conference, San Francisco, CA, June 2006.

[10]Maroney, D. R., Bolling, R. H., and R. Athale, A. D. C., "Experimentally Scoping the Range of UAS Sense and Avoid Capability," AIAA Paper 2007-2850, AIAA Infotech@Aerospace, Rohnert Park, CA, May 2007.

[11]Li, N. H. M., Liu, H. H. T., Earon, E. J. P., Fulford, C. D., Huq, R., and Rabbath, C. A., "Multiple UAVs Autonomous Mission Implementation on COTS Autopilots and Experimental Results," AIAA Paper 2009-5775, AIAA Guidance, Navigation and Control Conference, Chicago, IL, Aug. 2009.

[12]The Paparazzi Project, LLC, "Paparazzi," http://paparazzi.enac.fr/, Accessed Nov. 2012.

[13]3D Robotics, "APM — Open source autopilot," http://ardupilot.com/, Accessed Nov. 2013.

[14]PX4, "PX4 Autopilot Platform," https://pixhawk.ethz.ch/, Accessed Nov. 2013.

[15]Mahboubi, Z., Kolter, Z., Wang, T., and Bower, G., "Camera Based Localization for Autonomous UAV Formation Flight," AIAA Paper 2011-1658, AIAA Infotech@Aerospace, St. Louis, MO, Mar. 2011.

[16]Zafirov, D., "Autonomous VTOL Joined Wing UAV," AIAA Paper 2013-5087, AIAA Atmospheric Flight Mechanics Conference, Boston, MA, Aug. 2013.

[17]Moog Aircraft Group, "Moog Crossbow - The Smart Sensor Company - Super Smart," http://www.xbow.com/, Accessed Nov. 2013.

[18]RCAT Systems, "RCAT Systems - UAV & Unmanned Vehicle Products, UAV Telemetry System, UAV Electronics, Pitot Probes, Alpha Beta Probes," http://rcatsystems.com/uav.php, Accessed Oct. 2013.

[19]Eagle Tree Systems, LLC, "Eagle Tree R/C Telemetry," http://www.eagletreesystems.com/, Accessed Oct. 2013.

[20]Holly, L., Kowalchuk, S., Lederbogen, P., and Colgren, R., "University of Kansas UAV Dynamic Modeling and Flight Testing Development Program," AIAA Paper 2004-6541, AIAA Unmanned Unlimited, Chicago, IL, Sept. 2004.

[21]Antol, J., Chattin, R. L., Copeland, B. M., and Krizan, S. A., "The NASA Langley Mars Tumbleweed Rover Prototype," AIAA Paper 2006-64, AIAA Aerospace Sciences Meeting, Reno, NV, Jan. 2006.

[22]Johnson, B. and Lind, R., "High Angle-of-Attack Flight Dynamics of Small UAVs," AIAA Paper 2009-61, AIAA Aerospace Sciences Meeting, Orlando, FL, Jan. 2009.

[23]Johnson, B. and Lind, R., "Characterizing Wing Rock with Variations in Size and Configuration of Vertical Tail," *Journal of Aircraft*, Vol. 47, No. 2, 2010, pp. 567–576.

[24]Dantsker, O. D., Johnson, M. J., Selig, M. S., and Bretl, T. W., "Development of the UIUC Aero Testbed: A Large-Scale Unmanned Electric Aerobatic Aircraft for Aerodynamics Research," AIAA Paper 2013-2807, AIAA Applied Aerodynamics Conference, San Diego, CA, Jun. 2013.

[25]Higashino, S. I. and Sakurai, A., "A UAV Flight-Experiment System for the Estimation of Aerodynamic Characteristics," AIAA Paper 2003-6584, AIAA "Unmanned Unlimited" Conf. and Workshop & Exhibit, San Diego, CA, Sept. 2003.

[26]Beard, R. W., Kingston, D., Quigley, M., Snyder, D., Christiansen, R., Johnson, W., McLain, T., and Goodrich, M. A., "Autonomous Vehicle Technologies for Small Fixed-Wing UAVs," *Journal of Aerospace Computing, Information, and Communication*, Vol. 2, No. 2, 2005, pp. 92–108.

[27]Christophersen, H. B., Pickell, R. W., Neidhoefer, J. C., Koller, A. A., Kannan, S. K., and Johnson, E. N., "A Compact Guidance, Navigation, and Control System for Unmanned Aerial Vehicles," *Journal of Aerospace Computing, Information, and Communication*, Vol. 3, No. 2, 2006, pp. 187–213.

[28]Ippolito, C., Yeh, Y. H., and Kaneshige, J., "Neural Adaptive Flight Control Testing on an Unmanned Experimental Aerial Vehicle," AIAA Paper 2007-2827, AIAA Infotech@Aerospace, Rohnert Park, CA, May 2007.

[29]Jordan, T. L. and Bailey, R. M., "NASA Langley's AirSTAR Testbed: A Subscale Flight Test Capability for Flight Dynamics and Control System Experiments," AIAA Paper 2008-6660, AIAA Atmospheric Flight Mechanics Conference, Honolulu, HI, Aug. 2008.

[30]Brusov, V., Grzybowski, J., and Petruchik, V., "Flight Data Acquisition System for Small Unmanned Aerial Vehicle," Proceedings of the International Micro Air Vehicles, 't Harde, The Netherlands, Sept. 2011.

[31]Dantsker, O. D., Johnson, M. J., Akce, A. A., and Bretl, T. W., "Development of a Fixed Wing Multi-Role Unmanned Aircraft Vehicle Research Testbed," AIAA Paper 2012-0846, AIAA Aerospace Sciences Meeting, Nashville, TN, Jan. 2012.

[32]Dantsker, O. D., Mancuso, R., Caccamo, M., and Selig, M. S., "Robust Sensor Fusion for State Estimation on Agile Electric UAVs," Submitted to IEEE Real-Time Systems Symposium, Rome, Italy, Dec. 2014.

[33]Mancuso, R., Dantsker, O. D., Caccamo, M., and Selig, M. S., "A Low-Power Architecture for High Frequency Sensor Acquisition in Many-DOF UAVs," International Conference on Cyber-Physical Systems, Berlin, Germany, Apr. 2014.

[34]Hobbico, Inc., "Great Planes Avistar Elite .46 Advanced Trainer RTF," http://www.greatplanes.com/airplanes/gpma1605.html, Accessed Oct. 2013.

[35]Model motors s.r.o., "AXI 4120/14 GOLD LINE," http://www.modelmotors.cz/index.php?page=61&product=4120&serie=14&line=GOLD, Accessed Oct. 2013.

[36]Castle Creations, Inc., http://castlecreations.com/, Accessed Oct. 2013.

[37]Advanced Energy Tech, "Thunder Power RC," http://thunderpowerrc.com/, Accessed Nov. 2012.

[38]Hobbico, Inc., "Futaba Radio Control Systems and Accessories," http://futaba-rc.com/, Accessed Oct. 2013.